Extraction of Regions of Interest from Face Images Using Cellular Analysis

Arindam Biswas
Computer Science & Technology Dept.
Bengal Engineering & Science University
Shibpur, INDIA
91-03326686151
abiswas@cs.becs.ac.in

Suman Khara
Computer Science & Technology Dept.
Bengal Engineering & Science University
Shibpur, INDIA
91-03326686151
suman_khara@rediffmail.com

Partha Bhowmick
Computer Science & Technology Dept.
Bengal Engineering & Science University
Shibpur, INDIA
91-03326686151
partha@cs.becs.ac.in

Bhargab B. Bhattacharya
Advanced Computing & Microelectronics Unit
Indian Statistical Institute
Kolkata, INDIA
91-03325753003
bhargab@isical.ac.in

ABSTRACT
A novel algorithm for extracting the regions of interest (ROI) from face images is presented in this paper. The novelty of the algorithm comes from its *multi-resolution cellular analysis* coupled with an adaptive thresholding technique incorporating a unique idea of *exponential averaging*. The complexity of the cellular ROIs reported by the algorithm from the frontal face view as input, is further controllable by the chosen cell size, which is its added advantage. Apart from the actual ROIs representing the eye pair, nostrils, and the mouth area, some regions of non-interest may also creep in while extracting the set of cellular regions from the face image, which are discarded by a simple geometric analysis using a *containment tree*. The containment tree, which is newly introduced in this paper, captures the underlying relationship of the cellular regions, which, when analyzed, returns the face ROIs in an elegant representation. Since the entire algorithm works purely in the integer domain with primitive operations (comparison, right shift, and addition) only, it runs very fast for both gray-scale and color images. Some experimental results on different facial images demonstrate its speed, robustness, and efficiency.

Categories and Subject Descriptors
I.4.6 **[Segmentation] :** Edge and feature detection
I.4.10 **[Image Representation] :** hierarchical
I.4.7 [**Feature Measurement**]: size and shape

Compute 2008, Jan 18-20, Bangalore, Karnataka, India
?? 2008 ACM ISBN 978-1-59593-950-0 /08/01...$5.00

General Terms
Algorithms

Keywords
Face segmentation, region of interest, biometrics, adaptive thresholding, containment tree.

1. INTRODUCTION
As one of the most recent applications of image analysis and understanding in general, and biometric information management in particular, face recognition has received significant attention from the research community [21, 22]. Over the last few decades, face recognition has been widely applied in access control systems, model-based video coding, biometric identifications, etc. A face recognition system, in general, consists of the following steps: 1) face detection, 2) feature extraction, and 3) face recognition. Face detection deals with the problem of face localization [12, 15, 16]; feature extraction finds the presence of facial features like eyes, nose, nostrils etc. [5, 11, 13, 18]; and face recognition compares an input image against the database, and reports a match, if exists [2, 3, 17, 20].

In the diverse field of potential works related with human faces, face localization and facial feature extraction have been the two most important aspects. Accurate detection of the basic features as eyes, nose, and mouth is the most necessary prerequisite of most face recognition systems. There have been a number of face localization approaches, utilizing shape information (e.g., ellipse fitting method [10], mosaic images [14], color information [19], facial geometry and symmetry [1], etc). Also, there have been many facial feature extraction techniques, namely, eigenface approach [20], 2D Gabor wavelets [8], and discrete cosine transform (DCT) based approach [9].

In this paper, a novel algorithm for extracting the ROIs from face images, is presented. The algorithm uses an adaptive thresholding technique and exploits the simple geometric properties of a face. The major contributions of this paper may be listed as follows:

- the method is based on cellular analysis of a face image;
- the precision of the extracted ROIs can be controlled by varying the resolution level;
- the cost of computation is less as it involves only comparison, addition, and right-shift operations in the integer domain;
- the algorithm works for gray-scale as well as color face images.

The rest of the paper is organized as follows. Sec. 2 describes the proposed algorithm. Sec. 3 discusses the experimental results. Finally, we present the conclusion along with the future directions in Sec. 4.

2. PROPOSED WORK

In this paper, an algorithm is presented for extracting the regions of interest from gray-scale face images as well as color face images. In this two tier approach, first, the regions are extracted from the face image. Second, based on the region containment and the geometric relation of the face features the cellular regions representing the face and its features are obtained.

2.1 Face Localization

Given a gray-scale face image, J, and a cell size, c, the proposed algorithm extracts the face and its salient features in the form of cellular regions, such that c divides each edge length of each cellular region. The length and width of J is such that c divides both. Thus, J consists of an array of cells of size $c \times c$. Let α be a point in J, and let C_1, C_2, C_3, and C_4 be the four cells incident at α. Each such point, α, is classified as a vertex or otherwise, on the basis of face/object information of the four cells incident at α.

To determine whether a cell C_i has a portion of the face in it, a unique adaptive thresholding mechanism has been devised as follows. Let max_i and min_i denote the respective maximum and minimum gray level values in C_i. Then, the global maximum, max_g at α, is defined as the maximum of all max_is for i = 1,2,…, 4, corresponding to the four cells incident at α. Similarly, the global minimum, min_g, is defined as the minimum of all min_gs for i = 1,2,…,4. Based on max_g and min_g, we define the local threshold value at α as $\tau_{local} = 1/2\ (max_g - min_g)$. Then, the adaptive value of the threshold, τ_{adpt}, is computed in accordance with the following equation.

$$\tau_{adpt} = \gamma\, \tau_{local} + (1-\gamma)\, \tau_{prev} \qquad (1)$$

where, γ (in [0,1]) is the smoothing factor for the exponential moving average, and τ_{prev} is the adaptive threshold calculated for the previous point lying on the boundary of the cellular region.

If we expand the above equation further, we get:

$$\tau_{adpt} = \gamma\, \tau_{local} + (1-\gamma)\, \gamma\, \tau_{local}^{(1)} + \ldots + (1-\gamma)^i\, \gamma\, \tau_{local}^{(i)} + \ldots + (1-\gamma)^n\, \tau_0 \qquad (2)$$

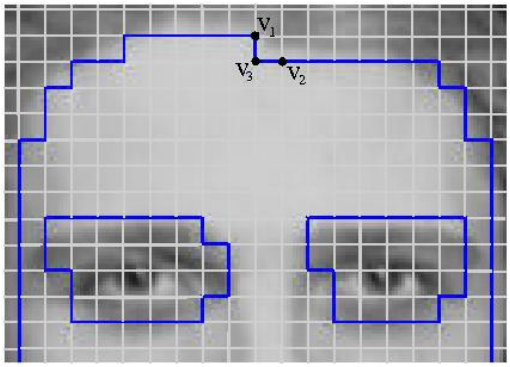

Figure 1: An example of different classifications of α

where, $\tau_{local}^{(i)}$ is the threshold value used in the last i^{th} classification, and τ_0 is the initial threshold.

It is evident from Eqn. 2 that, for γ = 1/2 , only the last eight threshold values contribute to the calculation of τ_{adpt} , since the gray value of a pixel in a gray-scale image is an 8-bit integer. The farther away they are from the current point along the boundary of the cellular region, the lesser effect they have on τ_{adpt}. As a result, apart from detecting a face cell that has more or less clear information, such a policy of considering the previous thresholds to determine the threshold enables a robust face localization. The algorithm becomes not only resilient to noisy data, if any, present in the image, but also insensitive to the variation of the illumination that often produces changing intensity across the image. Regarding issues related with the implementation of the aforesaid thresholding based on exponential averaging, certain significant points may be mentioned here. Realization of Eqn. 1 is computationally simplified if we consider γ = 1/2. For γ = 1/2, equal weightage is given to the threshold of the previous inter-cell point and the local contrast, and hence the computation of τ_{adpt} can be effected by a right shift operation only. However, for γ = 3/4, the above computation will involve floating point operation. Once the adaptive threshold, τ_{adpt}, for a given common point, α, is computed, then a cell C_i is said to contain a portion of the face, provided the following condition is satisfied:

$$\max_i - \min_i \geq \tau_{adpt} \qquad (3)$$

Thus, number of cells occupied by the object can be determined, and hence, the type of γ can be decided by checking the condition given in Eq. 3 for each cell surrounding α. Let n be the number of cells occupied by the face (or some face feature). Then, the following cases are possible:

i) Case C_0 (n = 0):
As none of the neighboring cells of α is occupied by the face, it is not a vertex of the ROI corresponding to the face.
ii) Case C_1 (n = 1):
Only one of the four cells incident at α has a part of the face; hence it qualifies to be a vertex with internal angle 90^0.
iii) Case C_2 (n = 2):

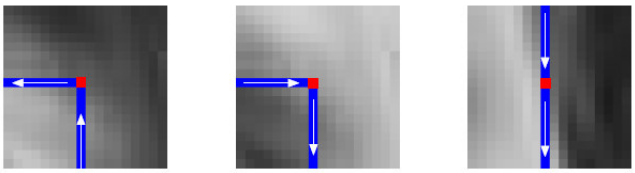

Figure 2: The incident edge versus outgoing edge relationship for 90^0 vertex, 270^0 vertex, and an edge point (180^0), considering that the face (brighter region in this instance) lies left during traversal of ROI.

If two adjacent cells are occupied, then α is an edge point; otherwise, if two opposite cells are occupied, then α is a 270^0 vertex.

iv) Case C_3 ($n = 3$):
Here, α is a 270^0 vertex as three cells are occupied.

v) Case C_4 ($n = 4$):
α is inside the face region and not a vertex.

Fig. 1 shows a portion of such a face image, where v_1 is a 90^0 vertex of the cellular region belonging to case C_1. Similarly, v_3 is a 270^0 vertex of the cellular region belonging to case C_3, and v_2 is a simple edge point.

2.2 Constructing the cellular regions

Let τ_0 (= 20 in our experiments) be the initial threshold value. For each (inter-cell) point, α, scanned in row major order, max_g and min_g are computed. If $max_g - min_g \geq \tau_0$, then α is assigned to be the start vertex, v_{start}. τ_{adpt} is computed using Eq. 1, taking $\tau_{prev} = \tau_0$ and the type of vertex is determined using Eq. 3. It is evident that v_{start} marks the start of a region only when it has sufficient contrast. It may be noted that, v_{start} is always chosen to be a 90^0 vertex, since there may arise a cellular region (e.g., a rectangle) in which a 270^0 vertex may not occur.

Assuming that the face lies left during traversal of the boundary of the cellular region, i.e., tracing the region boundary in anticlockwise sense, and v_{start} is the topmost (and leftmost) 90^0 vertex, the outgoing edge from v_{start} will be directed towards bottom. The outgoing edge traces to the next vertex, namely v_{next}. At v_{next}, max_is and min_is are computed corresponding to its four neighboring cells. Then, by applying Eqns. 1 and 3, the type of v_{next} is determined. The outgoing edge from any vertex is determined by the direction of the incident edge and the type of the vertex. A (inter-cell) point, which is traversed next, can be classified to one of three different types, namely, a 90^0 vertex, a 270^0 vertex, and an edge point. For the edge point, the outgoing edge direction remains the same as the incoming edge direction. However, for a 90^0 vertex, the traversal takes a left turn relative to the incident edge direction, (Fig. 2 (a)), and for a 270^0 vertex, the traversal takes a right turn (Fig. 2 (b)).

Thus, starting from v_{start}, the region boundary is traced to the next inter-cell point and its type is determined subsequently depending on the local gray level information associated with its four neighboring cells and the earlier thresholds concerned with the face region. Such a mechanism, therefore, makes a fast tracing procedure that encloses the face region in a cellular form by traversing its border points only. The traversal terminates and returns the ROI when it reaches v_{start}, which is ensured by our adaptive segmentation policy that incorporates the concept of coherent image information in an elegant way. The procedure is repeated to find the other cellular regions present in the image. As mentioned earlier, the construction of a cellular region is started from an inter-cell point only when sufficient contrast is found (Eq. 3).

2.3 Extraction of Regions of Interest

a priori knowledge about the face geometry is used. In order to identify the face feature regions from the set of extracted cellular regions as explained in Sec 2.2. The face, described by one cellular region, usually contains four more regions of interest inside it, which correspond to two eyes, the region of nostrils, and the mouth. The regions representing the eyes may have further subregions depending upon the characteristics of the face, (e.g., the eye brows may be separated from the eyes depending on the cell specification). In fact, for a frontal face image, the center of the two regions representing the pair of eyes will approximately lie on the same horizontal line. Also, the center of the nostril region and that of the mouth region lies approximately on the vertical axis (of symmetry) that passes through the center of the face region. Following the above characteristics, the four regions inside the face region can be characterized. These regions are considerably smaller in size compared to the face region. More importantly, these regions can be studied in detail for subsequent works, e.g. for designing an efficient face recognition system.

Region containment tree

The region extraction algorithm works in a way such that, for each pair of regions R_i and R_j , where R_i is discovered before discovering R_j , we have either $R_j \subset R_i$ (containment property) or $R_i \cap R_j = \emptyset$. For each new region R_j , we check its containment with the previously discovered regions, $\{R_i : 1 \leq i \leq j - 1\}$, using a geometric procedure. If a vertical ray, directed upwards (or downwards) and passing through some vertex v_j of R_j , intersects (the boundary of) R_i an odd number of times, and a horizontal ray, directed rightwards (or leftwards) and passing through v_j , also intersects R_i an odd number of times, then v_j (and R_j , thereof) lies inside R_i. If R_j lies inside R_i, then the node corresponding to the former becomes the child node corresponding to the latter in the containment tree, T. Further, for multiple regions R_{j1}, R_{j2} …, contained in a particular region R_i, the corresponding nodes are placed in T such that the left-to-right ordering of the sibling nodes preserve the left-to-right and top-to-bottom arrangement of R_{j1}, R_{j2} … in R_i. For example, if the leftmost (topmost) vertex of R_{j1} lies to the left (top) of the leftmost (topmost) vertex of R_{j2}, then the node corresponding to R_{j1} occurs to the left of the node corresponding to R_{j2} in T.

Fig. 3 illustrates the proposed scheme. The cellular regions extracted from the given face image are six in number (Fig. 3(b)). The region containment tree is constructed from these six regions, as depicted in Fig. 4. As the algorithm extracts the nonintersecting cellular regions one by one, the region containment tree (denoted by T) is built as follows.

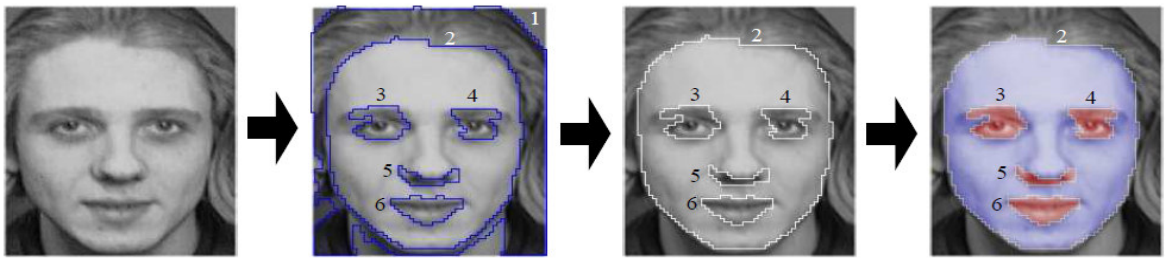

Figure 3: The steps of the proposed scheme are shown here. (a) original image (b) extracted cellular regions (c) the outermost region, marked as '1' is dropped on the basis of known geometric features of the face (by analyzing the containment tree, Fig. 4), and (d) finally extracted regions of interest are shaded as '3','4','5', and '6'.

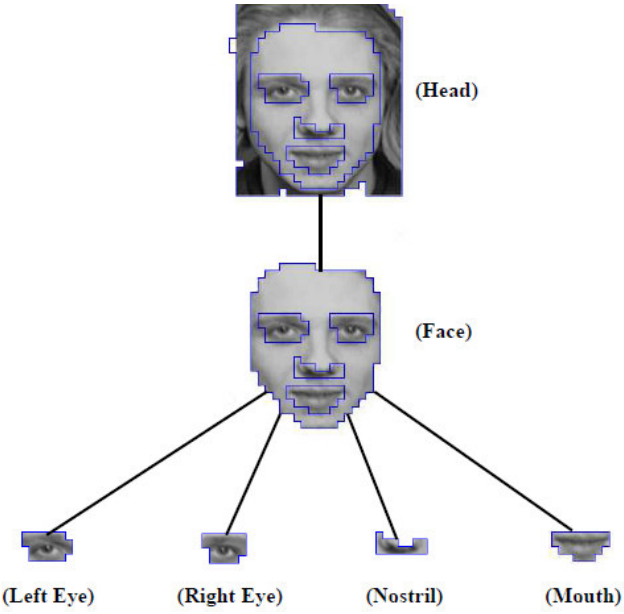

Figure 4: The region containment tree corresponding to a face image.

The first cellular region, extracted by the algorithm, is marked by '1', which is assigned as the first node of *T*. Since the next region, namely region '2', lies entirely inside region '1', the node '2', corresponding to region '2' (face region), is inserted as a child of node '1' in *T* . Region '2', in turn, contains four other regions, namely, '3', '4', '5', and '6', whose centers are computed. Then these four regions are checked w.r.t. the line of symmetry of the face and their relative positions. The line of symmetry of the face is given by $x = (x^{(2)}_{min} + x^{(2)}_{max})/2$, where $x^{(2)}_{min}$ and $x^{(2)}_{max}$ represent the respective minimum and maximum *x*-coordinates of region '2'. We consider a tolerance parameter δ (= 5) to check the approximate correctness of locations of the four regions w.r.t. region '2'. The centers of '3' and '4' should lie approximately on the same horizontal line (i.e., the vertical distance between their centers should not differ by more than δ, whereas those of '5' and '6' should lie approximately on the line of symmetry of the face.

Thus, it is concluded that region '2' represents the face region, '3' and '4' represent the two eye regions, whereas '5' and '6' represent the nostril region and the mouth region respectively. Any other extracted cellular region (possibly corresponding to scar, mole, etc.) not satisfying the above-mentioned conditions is not considered as a part of the containment tree.

It is evident from the process of construction of the cellular regions that, varying the cell size, *c*, a crisper or coarser description of the regions of interest can be obtained. This multiscale treatment of a given image is illustrated in Fig. 6. For cell size, $c = 8$, a gross description of the regions of interest are obtained, whereas for $c = 2$, it extracts the finer descriptions of eyes, nostril area and the mouth region.

2.3.1 Region Merging

The containment tree is also used by us to take care of some infrequent cases in which the face region contains more than four cellular regions. The underlying geometric relation of the cellular regions captured in the containment tree, is used to merge (and label) two or more regions contained in the face region, in order to extract the face ROIs. For example, the face region (2) in Fig. 5 contains six cellular regions (3, 4, 5, 6, 7, and 8). One pair of (vertically symmetric) regions lies above the other pair, the former representing the eye-brows and the latter representing the eyes. Regions 3 and 4, representing the eye-brows, are merged with the regions 5 and 6, representing the eyes, respectively as follows.

Let $R1$ and $R2$ be two cellular regions whose respective minimum and maximum *x* and *y* coordinates are $(x^{(1)}_{min}, x^{(1)}_{max})$, $(y^{(1)}_{min}, y^{(1)}_{max})$, $(x^{(2)}_{min}, x^{(2)}_{max})$ and $(y^{(2)}_{min}, y^{(2)}_{max})$. Let, w.l.o.g., $y^{(1)}_{max} > y^{(2)}_{max}$, which implies R_1 lies above R_2. Then R_1 and R_2 are merged to a single ROI if the following condition is true.

$$y^{(1)}_{min} - y^{(2)}_{max} < 20 \text{ and}$$

$$| x^{(1)}_{min} - x^{(2)}_{min} | < 10 \text{ and } | x^{(1)}_{max} - x^{(2)}_{max} | < 10$$

For merging R_1 and R_2, we consider their minimum and maximum x-coordinates. If $x^{(1)}_{min} \geq x^{(2)}_{min}$, then the point of R_1 having $x = x^{(1)}_{min}$ and minimum *y*-coordinate is joined with the point of R_2 having $x = x^{(1)}_{min}$ and maximum *y*-coordinate. The merging of the eyes and their eyebrows in Fig. 5 illustrates this case. Similarly, if

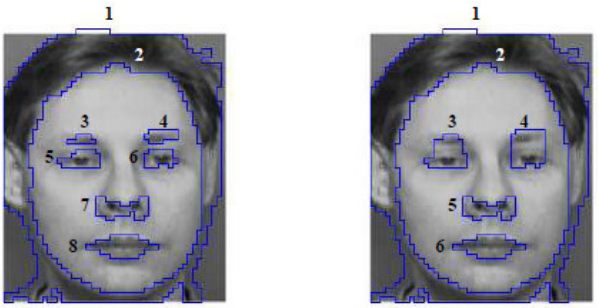

Figure 5: Region Merging. Left: before merging. Right: after merging the eyes and the corresponding eyebrows.

$x^{(1)}_{min} < x^{(2)}_{min}$, then R_1 and R_2 are joined by considering the appropriate points on their border. Merging is also done in a similar manner from the right ends of the two regions.

2.4 Color Images

The above technique is extendable to color face images also. The color image is considered in the RGB format. Three different thresholds, adaptive in nature, are computed corresponding to the three color components as the region construction progresses as per Eq. 1. The containment of the face information in the cell is determined using Eq. 3 for each of the three color components, and if at least one color component signifies the presence of the face in cell, then the corresponding cell is said to be containing a portion of the face. Once the type of the inter-cell point is determined, the construction of the region is done in a similar manner as in the case of a gray-scale image, explained in Sec. 2.2.

It is to be noted here that the complexity of the algorithm depends on the perimeter of the regions of the face and face features and also on the cell size c. It is clear that for a lower value of c, the extracted regions have higher number of vertices and edges, whose computation time is high. The computation time, however, decreases as c is increased, since it produces lesser number of vertices and edges of the extracted regions. Run-time of the algorithm is, therefore, controllable by adjustment of c, which is reflected in the results given in Sec. 3.

3. RESULTS AND DISCUSSIONS

The proposed algorithm for extracting the regions of interest of a face image has been tested on various face images, and the extended version has been tested also on a set of color images. The proposed algorithm has been implemented in C on a Sun Ultra 5 10, Sparc, 233 MHz, the OS being SunOS Release 5.7 generic. The databases used are the Database of Faces from AT&T Laboratories, Cambridge [6] for gray-scale images and the MIT-CBCL Face Recognition Database [7] for color images. The results of the gray-scale faces are shown in Fig. 7 and those of the color images in Fig. 8.

Table 1 shows the CPU time required for extraction of ROIs in gray scale images as well as color images for different cell sizes. As the algorithm operates entirely in the integer domain, no floating point operation being involved, it executes very fast, which is evident from the times shown in the table. It is also seen that the time required decreases drastically with higher cell sizes.

Table 1: CPU Times required for extraction of ROIs in seconds.

Image name	Size($rows \times cols$)	c	CPU Time
man1 (gray-scale)	248 × 288	2	0.055
		4	0.046
		8	0.033
man2 (gray-scale)	248 × 288	2	0.057
		4	0.049
		8	0.037
man (color)	392 × 320	2	0.071
		4	0.064
		8	0.052
lady (color)	392 × 320	2	0.067
		4	0.056
		8	0.047

The time required for color images are higher than that for gray-scale images, since the analysis works on three color components (RGB).

4. CONCLUSION AND FUTUREWORKS

In this paper, we have presented a novel algorithm for extracting the regions of interest from frontal face images. The algorithm is uniquely featured by the cellular representation of its reported ROIs, whose complexity (i.e., number of vertices) is further controlled by the adopted cell size, thereby imparting the desired level of precision depending on the subsequent application. A unique adaptive thresholding mechanism for gray-scale image, which can be also extended to color images, has been incorporated to make the algorithm robust and efficient. A simple yet novel data structure, called containment tree, has been proposed to extract and to correlate the face region and its features. This has been tested on different databases with encouraging results, some of which are presented in this paper. Presently, we are working on preparing the results compared to other ROI extraction techniques. We are also working on designing a face identification system on the basis of the extracted regions of interest, which will be reported in future.

5. REFERENCES

[1] R. Brunelli and T. Poggio, Face Recognition: Features versus Templates, IEEE Trans. PAMI, vol. 15, no. 10, pp. 1042-1052, 1993.

[2] K. I. Chang, K. W. Bowyer, and P. J. Flynn, Multiple Nose Region Matching for 3D Face Recognition under Varying Facial Expression, Proc. First Intl. Workshop Automatic Face and Gesture Recognition, vol. 28, no. 10, pp. 1695-1700, 2006.

[3] R. Chellappa, C.L. Wilson, and S. Sirohey, Human and Machine Recognition of Faces: A Survey, Proc. IEEE, vol. 83, no. 5, pp. 705-740, 1995.

[4] C.W. Chen, J. Luo, and K.J. Parker, Image Segmentation via Adaptive K-mean Clustering and Knowledge-based Morphological Operations with Biomedical Applications. IEEE Trans. Image Processing, vol. 7, no. 12, pp. 1673 - 1683, 1998.

[5] I. Craw, D. Tock, and A. Bennett, Finding Face Features, Proc. Second European Conf. Computer Vision, pp. 92-96, 1992.

[6] http://www.cl.cam.ac.uk/Research/DTG/attarchive:pub/data/-

att faces.tar.Z. AT&T \The Database of Faces" (formerly \The ORL Database of Faces"). AT&T Laboratories, Cambridge.
[7] http://cbcl.mit.edu/software-datasets/heisele/ facerecognition-Database.html. MIT-CBCL Face Recognition Database.
[8] B. Duc, S. Fisher, and N. J. BigÄun, Face authentication with Gabor information on deformable graphs, IEEE Trans. Image Proc., vol. 8, no. 4, pp. 504-516, 1999.
[9] S. Eickler, S. MÄuller, and G. Rigoll and A. Jacquin, Recognition of JPEG compressed face images based on statistical methods, Image Vis. Comput., vol. 18, no. 4, pp. 279 - 287, 2000.
[10] A. Eleftheriadis and A. Jacquin, Automatic face location, detection and tracking for model-assisted coding of video teleconferencing sequences at low-bit rates, Signal Processing: Image Communication, vol. 7, no. 3, pp. 23-248, 1995.
[11] H.P. Graf, T. Chen, E. Petajan, and E. Cosatto, Locating Faces and Facial Parts, Proc. First Int· Sl Workshop Automatic Face and Gesture Recognition, pp. 41-46, 1995.
[12] M. Hamouz and J. -K. Kamarainen and P. Paalanen, Feature-Based Affine-Invariant Localization of Faces, IEEE TPAMI, vol. 27, no. 9, pp. 1490-1495, 2005.
[13] Yea-Shuan Huang and Hao-ying Cheng and Po-Feng Cheng and Cheng-Yuan Tang, Face Detection with High Precision Based on Radial-Symmetry Transform and Eye-Pair Checking, Proceedings of the IEEE Intl. Conf. Video and Signal Based Surveillance, pp. 62-67, 2006.
[14] C. Kotropoulos, I. Pitas, S. Fische, and B. Duc Face Authentication Using Morphological Dynamic Link Architecture, Proc. AVBPA'97, pp. 169-176, 1997.
[15] K. Lam and H. Yan, Fast Algorithm for Locating Head Boundaries, Electronic Imaging, vol. 3, no. 4, pp. 351-359, 1994.
[16] B. Moghaddam and A. Pentland, Probabilistic Visual Learning for Object Recognition, IEEE TPAMI, vol. 19, no. 7, pp. 696-710, 1997.
[17] A. Samal and P.A. Iyengar, Automatic Recognition and Analysis of Human Faces and Facial Expressions: A Survey, Pattern Recognition, vol. 25, no. 1, pp. 65-77, 1992.
[18] P. Sankaran and S. Gundimada and R. C. Tompkins and V. K. Asari, Pose Angle Determination by Face, Eyes and Nose Localization, Proceedings of the 2005 IEEE Computer Society Conference on Computer Vision and Pattern Recognition (CVPR'05) - Workshops, pp. 161-168, 2005.
[19] K. Sobottka, and I. Pitas, A novel method for automatic face segmentation, facial feature extraction and tracking, Signal Processing: Image Communication, vol. 12, no. 3, pp. 263-281.
[20] M. Turk and A. Pentland, Eigenfaces for Recognition, J. Cognitive Neuroscience, vol. 3, no. 1, pp. 71-86, 1991.
[21] M.H. Yang, D.J. Kriegman, and N. Ahuja, Detecting Faces in Images: A Survey, IEEE TPAMI, vol. 24, no. 1, pp. 34-58, 2002.
[22] W. Zhao, R. Chellappa, P. J. Phillips, and A. Rosenfeld, Face Recognition: A Literature Survey, ACM Computing Survey, vol. 35, no. 4, pp. 399-458, 2003.

Figure 6: Regions of interest of a given image for different cell sizes.

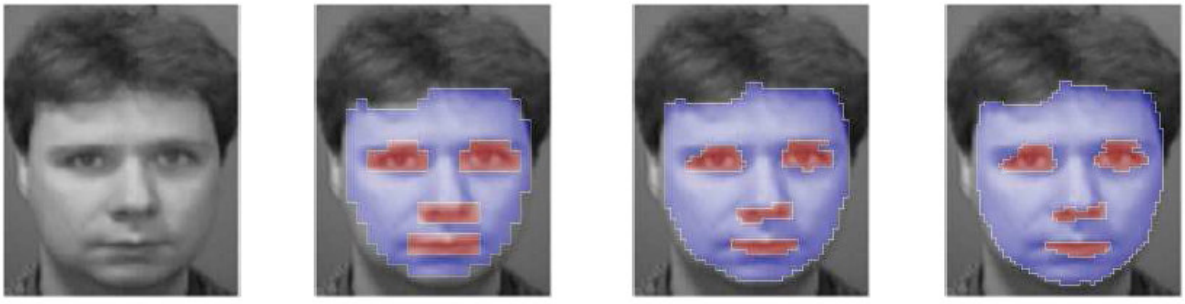

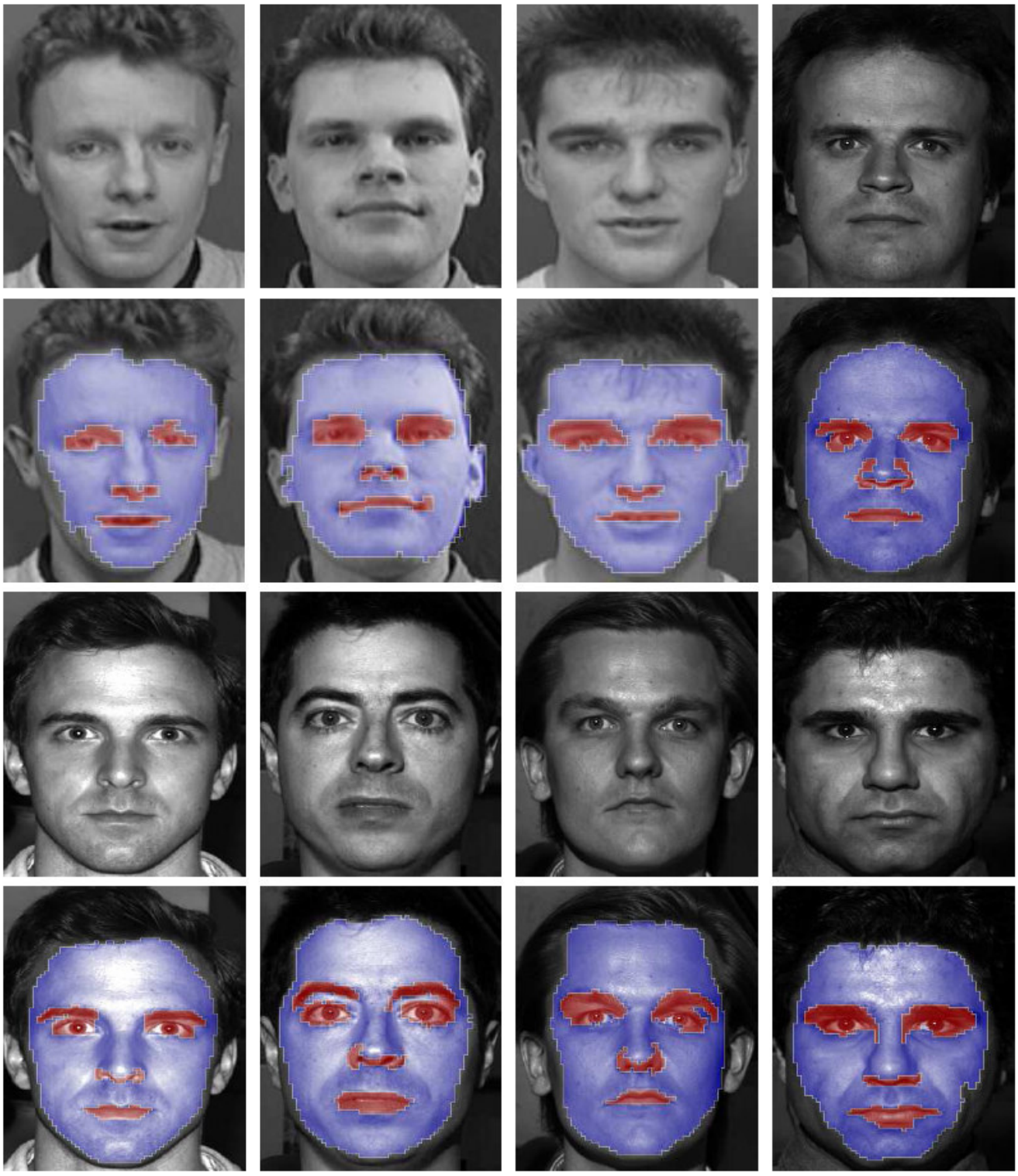

Figure 7: 1st and 3rd rows show the original gray-scale images; 2nd and 4th rows show the corresponding outputs.

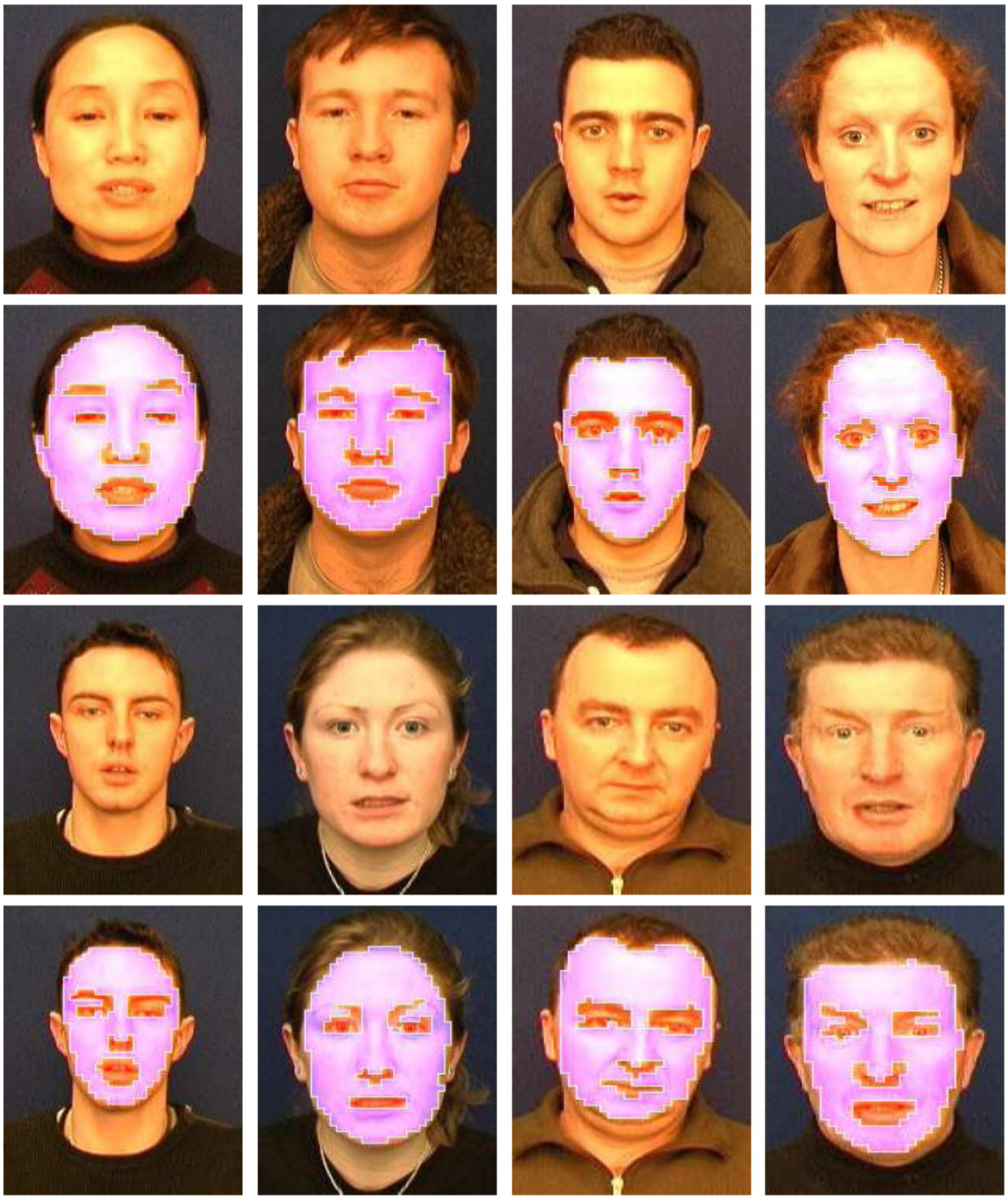

Figure 8: 1st and 3rd rows show the original color faces; 2nd and 4th rows show the corresponding outputs.